Research Journal of Chemical Sciences _____ ISSN 2231-606X
Vol. **5(1),** 33-40, January **(2015)** *Res. J. Chem. Sci.*

Structural, Optical, Thermal and Electrical properties of Fungus guided Biosynthesized Zinc Sulphide Nanoparticles

Senapati U. S.[1*], Jha D.K.[2] and Sarkar D.[3]
[1]Department of Physics, Handique Girls' College, Guwahati-781001, INDIA
[2]Department of Botany, Gauhati University, Guwahati-781014, INDIA
[3]Department of Physics, Gauhati University, Guwahati- 781014, INDIA

Available online at: www.isca.in, www.isca.me
Received 15th December 2014, revised 26th December 2014, accepted 15th January 2015

Abstract

A green synthesis approach to the fabrication of zinc sulphide (ZnS) nanoparticle is carried out using the extract of button mushroom (Agaricus bisporus), a naturally occurring edible mushroom. The XRD analysis show that ZnS nanoparticles are of cubic structure with average crystallite size of 2.9 nm – 2.1 nm which is in good agreement with the data found from TEM analysis. Direct band gap of the samples is estimated from UV-Vis absorption and found to lie in the range of 4.9eV-5.3eV. Photoluminescence (PL) of the samples is due to the presence of zinc vacancies and recombination of electron-hole pair at the surface traps of the materials. The FTIR study confirms the presence of protein, the guiding material for biosynthesis of nanomaterial. The thermal stability of the samples is studied with thermogravimetric analysis (TGA). Impedance analysis of the samples reveals the potential applications of the materials in nanotuned devices.

Keywords: Biosynthesis, ZnS, FTIR, TGA, Impedance analysis.

Introduction

Nanotechnology has attracted global attention because the nano-materials have properties unique from their bulk equivalents. Among the various class of nonmaterial, semiconductor ZnS are witnessing extreme attention due to their interesting properties and applications[1,2]. ZnS nanoparticles can be synthesized using various physical and chemical methods[3,4]. However, most of these methods are based on high-temperature, and/or high pressure, radiation and on the use of toxic chemicals, namely H_2S as the sulphide source or evolve toxic materials. Currently, there is a growing need to develop environment friendly nanoparticles that do not produce toxic wastes in their synthesis protocol. Biological methods for nanoparticle synthesis using microorganisms, enzyme and plants or plant exudates have been suggested as possible ecofriendly alternatives to chemical and physical methods[5]. Biological synthesis of semiconductor ZnS nanoparticles using bacteria has been carried out by several earlier workers. To name a few, H.J.Bai et al.[6] prepared ZnS nanoparticles using immobilized *Rhodobacter sphaeroides* while C. Malarkodi et al.[7] used *Serratia nematodiphila* for this purpose.

Compared to bacteria, fungi are known to secrete much higher amount of proteins, thus might have significantly higher productivity of nanoparticles in biosynthesis approach[5]. Mushrooms are the fleshy, spore-bearing fruiting body of a fungus, typically produced above ground on soil or on its food source. Mushrooms are known to have antioxidant, antimicrobial, anti-inflammatory, antitumor and anticancer activities[8]. It is well known that mushrooms are rich in proteins, vitamins and amino acids. There are reports on the synthesis of nanoparticles using edible mushroom. For example, D. Dhanasekaran et al.[9] have used *Agaricus bisporus* extract for the synthesis of silver nanoparticles, D.Philip[8] has used *Volvariella volvacea* extract for the synthesis of Au, Ag and Au-Ag nanoparticles and R.Bhat et al.[10] have used *Pleurotus florida* extract for the synthesis of gold nanoparticles . Though biosynthesis of ZnS nanoparticles is very much the need of the hour, extensive work in this area is yet to be done. In our earlier work[2] we have studied the structural and optical properties of synthesized ZnS nanoparticles using *Pleurotus ostreatus* (oyster mushroom) extract. In this present work, we have studied the structural, optical and the variation of admittance (impedance) with frequency of the synthesized ZnS nanoparticles using a new fungus namely *A. bisporus* (button mushroom). To the best of our knowledge button mushroom is not used for the synthesis of ZnS nanoparticles. The importance of this button mushroom over oyster mushroom is that button mushroom is the most common and is cultivated worldwide and totally accounts for 38% of the world edible mushroom[11]. We also compare the present work results with our earlier work [2] results.

Material and Methods

Materials used for the synthesis of ZnS nanoparticles in the present work are mushroom, $ZnCl_2$ and Na_2S. Fresh button mushroom (*A. bisporus*) is obtained from Millanjyoti Firm, Guwahati (SSI Reg. No: 180610838). $ZnCl_2$ and Na_2S are Zinc source and Sulphur source respectively. These are obtained from Merck Specialities Private Ltd. and Qualigens fine chemicals respectively and used without any further purification.

For the purpose of mushroom extract similar process has been followed as has done in our recent work for oyster mushroom[2]. To be particular, 100g fresh button mushrooms are washed repeatedly with distilled water to remove any organic impurities present on it. The cleaned mushrooms are then cut to small pieces with a sterilized knife. The small pieces of mushrooms are then boiled for 10min in 500ml distilled water and filtered. The filtrate is cooled to room temperature. The resultant filtrate is the extract of mushroom and used as capping agent and stabilizer for the preparation of ZnS nanoparticles.

For the preparation of ZnS nanoparticles a solution of 1M $ZnCl_2$ is prepared in 100ml of deionised water and solution of 1M Na_2S is prepared in 100ml deionised water. The solution of Na_2S is added drop wise to the prepared $ZnCl_2$ solution and then mushroom extract is added drop wise to the mixture, which is kept on stirring at 70°C. The resultant solution is kept at room temperature overnight to complete the reaction which results in formation of ZnS nano colloids. The amounts of mushroom extract used are 50ml, 100ml and 150ml to obtain three varieties nanocolloids. The nano particles are collected after centrifugation of the colloid at 2,000 rpm for 15min. The resultant product is dried at 120°C for 2 hours and then crushed to fine powder with the help of mortar and pestle. We name these samples obtained for different volume of the extract (50, 100 and 150 ml) as A, B and C respectively.

Characterization of ZnS nanoparticles: Prepared ZnS nanoparticles are examined by XRD technique using an X-ray diffractometer (Philips X'pert-with CuKα radiation) of wavelength 0.154 nm over 2θ range of 20^0-80^0. The purity and elemental analyses of the samples are examined by EDAX (Oxford, INCA-7587). SEM images are obtained using JEOL, JAPAN-JSM-6360. TEM micrographs are obtained in JEOL JEM 2100 using an accelerating voltage of 200 KV. UV-Visible spectra are recorded in a Hitachi U-3210 spectrometer, PL spectra are recorded by Hitachi F-2500 and FTIR spectra are recorded by Perkin Elmer Spectrum RXI FTIR system. Impedance analysis of the samples is examined by LCR Hitester HIOKI 3532, TGA analysis is carried out by perkin Elmer SDT 600.

Results and Discussion

Structural analysis: Figure-1 shows XRD patterns of samples A, B and C synthesized by using various amount of *A. bisporus* extract. Three broad peaks are observed in the diffractrogram at around 28.54^0, 47.73^0, 56.28^0 for Sample A. These peaks correspond to cubic lattice structure of ZnS and assigned to the planes (111), (220) and (311) respectively. With increase of the amount of mushroom extract (samples B and C), these peaks are seen to be shifted marginally with increase of peak broadening suggesting decrease of particle size with increasing mushroom extract. It is also to be noted that no diffraction peaks from other crystalline forms are detected, indicating high purity and well crystalline of the obtained ZnS particles. Also, the broadening of the XRD patterns indicates the nanocrystalline nature of the samples. The crystallite size is calculated using Debye-Scherrer formula[2]:

$$D = \frac{K\lambda}{\beta \cos\theta},$$

Where D is the crystallite size, K is the geometric factor (0.98), λ is the X-ray wavelength ($1.54A^0$), β is the full with at half maxima (FWHM) of the diffraction peaks (radian) and θ is the diffraction angles. The average crystallite size is found to vary in the range of 2.9 nm- 2.1 nm for these samples with decreasing trend as the amount of extract is increased.

The value of interplanar spacing (d) is calculated using the expression[1]:

$d_{hkl} = \frac{n\lambda}{2\sin\theta}$ and the lattice constant (a) of the synthesized cubic zinc blend is calculated using the relation[12]:

$$a = d\sqrt{h^2 + k^2 + l^2},$$

Where h, k and l are the Miller indices for the respective planes. The calculated lattice constants are slightly different for different orientations of the same sample. The deviation in the values of the lattice constant from the bulk value ($5.42A^o$) indicates the presence of strain in the samples. Hence, an attempt has been made to estimate the average strain (ε_{str}) of the ZnS nanoparticles using Stokes-Wilson equation[2]:

$$\varepsilon_{str} = \frac{\beta}{4\tan\theta}$$

Where β is the FWHM and θ is the diffraction angle.

The strains in turn are related to the dislocations developed in the crystals. The dislocation density (δ) which represents the amount of defects in the sample is determined using the formula suggested by Williamson and Smallman[2]:

$$\delta = \frac{1}{D^2}$$

Where D is the average crystallite size.

The structural properties are displayed in table-1 to have ready comparison. It is clear from this table that average crystallite size decreases with increase of the volume of *A. bisporus* extract. This decrease in crystallite size in turn leads to increase of dislocation density and average strain. It indicates smaller crystallites incorporate more imperfections as dislocations are nothing but one form of imperfection[13].

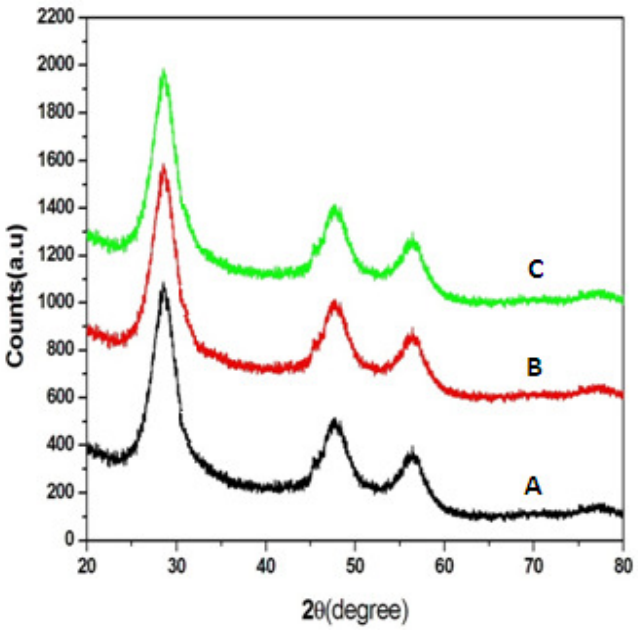

Figure-1
XRD Patterns of ZnS nanoparticles

Table-1 Structural Properties of ZnS nanoparticles

Sample	2θ(^{0})	*D*(nm)	*d* (A^0)	*a*(A^0)	$\mathcal{E}_{str}$ x10^{-3}	δx10^{16} lines/m^2
A	28.54 47.73 56.28	2.9	3.13 1.90 1.63	5.43 5.37 5.40	43	11.8
B	28.47 47.91 56.51	2.5	3.13 1.89 1.62	5.43 5.34 5.37	45	16.0
C	8.47 7.55 6.51	2.1	3.14 1.91 1.63	5.43 5.40 5.40	46	22.6

Elemental analysis: For elemental analysis of the synthesized ZnS nanoparticles, we have carried out EDAX study of one representing sample (A) as the study reveals similar nature for all the samples. This is shown in figure-2. This confirms the presence of Zinc and sulphur. Along with these other elemental signals C and O are recorded, these have possibly come from unreacted proteins or enzymes of the *A. bisporus* extract. Similar results have been obtained in our earlier work[2] as well as by M.Hudlikar et al.[14]. The average atomic percentage ratio of Zn:S is found to be 48.78:50.63 which is very close to the theoretical expectation of 1:1.

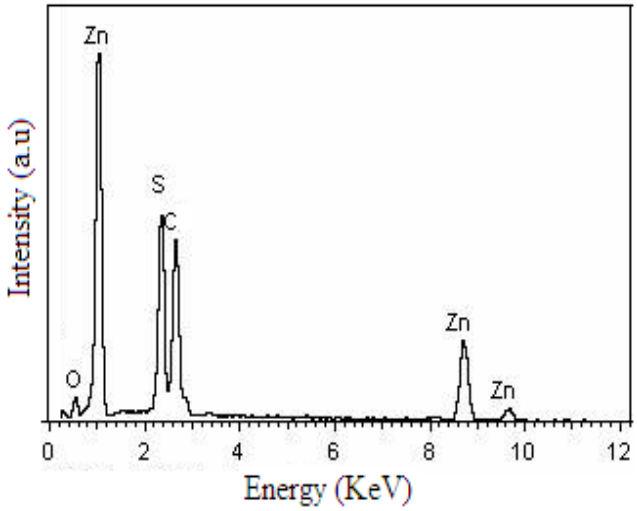

Figure-2
EDAX Pattern of sample A

Morphology analysis: The morphology of the samples is studied from SEM images. These images for the three samples are shown in figure-3. It is clear that the volume of *A. bisporus* extract has an obvious effect on the surface morphology of the samples. SEM results reveal that the particles are agglomerated in samples A, B and C. But it is evident from the SEM image that the agglomeration as well as particle size is decreasing with the increase of the *A. bisporus* extract volume (from sample A to C). With high extract volume (150 ml) the SEM image of the sample C shows almost spherical shaped nanoparticles. However, the actual size cannot be determined by SEM due to the limitation of the resolution of the instrument.

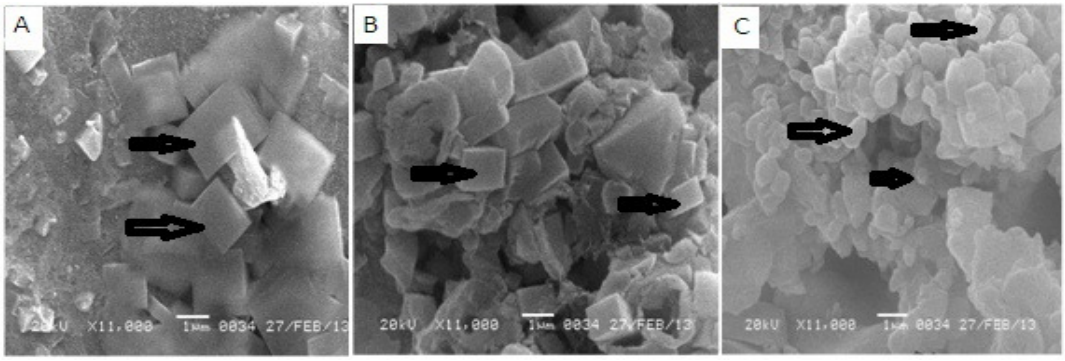

Figure-3
SEM images of samples A, B and C

TEM study: Figure-4 shows the TEM images of samples A, B and C. These indicate that the samples are composed of a large quantity of nanoparticles with spherical shape. The average particle size is found to vary from 3.5 nm – 2.1 nm and it is found to decrease gradually as the volume of extract increases. This is in good agreement with that calculated from XRD. The presence of *A. bisporus* extract causes strong interaction between the protective bio molecules and the surfaces of the nanoparticles preventing ZnS nanoparticles from sintering[2]. With larger quantity of extract the interaction is intensified, leading to size reduction of spherical nanoparticles[8]. The Selected Energy Diffraction (SAED) patterns (insets of figure-4) show concentric rings instead of sharp spots. These diffuse rings indicate the polycrystalline nature of the material. The rings have been indexed to (111), (220) and (311) planes of the cubic ZnS phase (JCPDS File no.5-0566) that are corresponding to d (111) =3.1114A^o , d (220) =1.904A^o and d (311) =1.6277 A^o, respectively, confirming the presence of cubic ZnS[14].

UV-Visible Spectra: Figure 5(a) shows the UV-Visible absorption spectra of ZnS nanoparticles A, B and C. The absorption peaks exhibit blue shift and strong intensity. Such a strong peak is known to arise due to quantum confinement effect, which occurs when the particle size becomes comparable with or smaller than the Bohr radius of excitation[15].

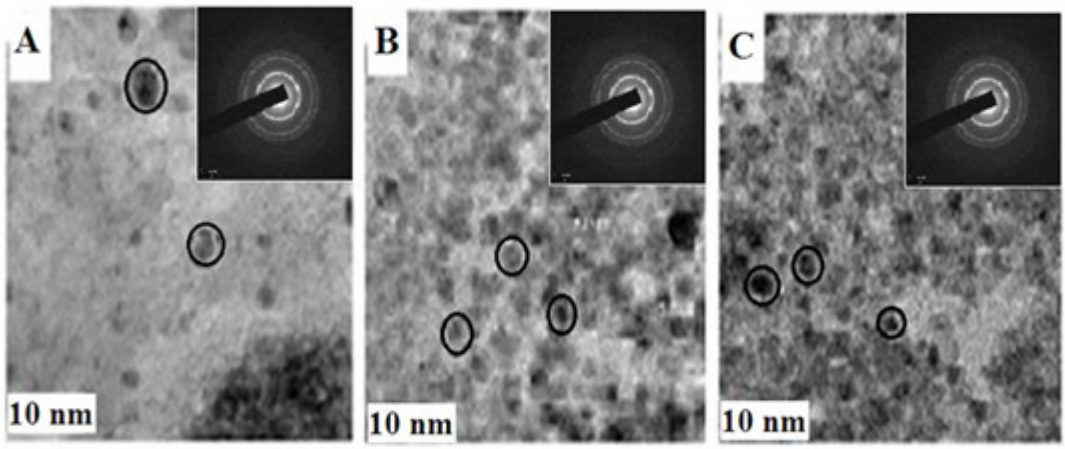

Figure-4
TEM image of samples A, B and C

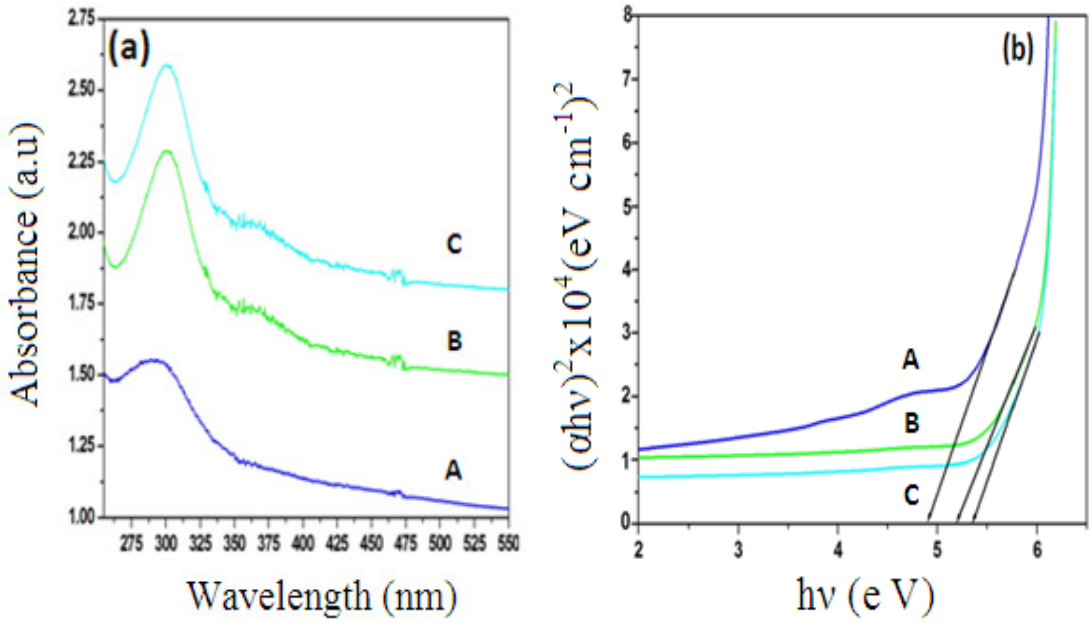

Figure-5
(a) UV-Vis spectra and (b) Calculation of optical band gap from UV-Vis

The relation between the incident photon energy ($h\nu$) and the absorption coefficient (α) is given by the relation[16]: $(\alpha h\nu)^{\frac{1}{m}} = C(h\nu - E_g)$, where C is constant and E_g is the band gap of material and exponent m depends on the type of transition. For direct allowed transition m= ½, for indirect allowed transition m = 2, for direct forbidden m=3/2 and for indirect forbidden m = 3. Direct band gap of the samples are calculated by plotting $(\alpha h\nu)^2$ vs $h\nu$ and then extrapolating the liner portion of the curve on $h\nu$ axis at $\alpha = 0$, shown in Figure 5 (b). The optical band gap of the samples is found to lie in the range of 4.9 *eV*- 5.3 *eV*. The obtained band gap values are higher than that of the bulk value (3.7*eV*) owing to quantum confinement effect[12]. From the blue shifted absorption edge, the particle size has been calculated using the formula[2]:

$$E_{gn} = sqrt\left[E_{gb}^{2} + \left\{ 2h^{2} E_{gb} \frac{\left(\frac{\Pi}{R}\right)^{2}}{m^{*}} \right\} \right]$$

Where, R is the radius of the particle size, E_{gb} is the band gap of the bulk material, E_{gn} is the band gap of the nano material, h is the Planck's constant and m^* is the effective mass of the specimen (3.64×10^{-31} kg for ZnS). The estimated particle size of the samples is found to be 7.2 nm-6.1 nm. It is seen that the partice size is decreasing with increasing volume of the *A. bisporus* extract. This is in good agreement with that calculated from XRD, SEM and TEM. The refractive index of the samples A, B and C are calculated using the relation[17]:

$n^4 E_g = 59\ eV$,

Where n is the refractive index and E_g is the band gap of the sample.

The optical properties are given in table-2. It is observed that with increasing volume of the extract the band gap increases whereas the refractive index decreases.

Table-2
Optical properties of ZnS nanoparticles

Sample	Band gap(eV)	Particle Size(nm)	Refractive Index
A	4.9	7.2	1.86
B	5.2	6.3	1.83
C	5.3	6.1	1.81

Photoluminescence (PL) Study: Figure-6 shows the room temperature photoluminescence spectra of ZnS nanoparticles A, B and C for excitation wavelength of 280 nm. These shows peaks centred at 358 nm. In the previous studies of colloidal ZnS nanoparticles the authors reported that higher electrons levels are expected for zinc vacancies[2]. Therefore, we attribute the 358 nm peaks to zinc vacancies. The PL spectra of all the ZnS samples show a weak shoulder at around 440 nm. The origin of this shoulder at lower energy compared to the main peak can be attributed to the recombination of electron-hole pair at the surface traps, which arises for higher surface to volume ratio of the nanoparticles due to their small size[18].

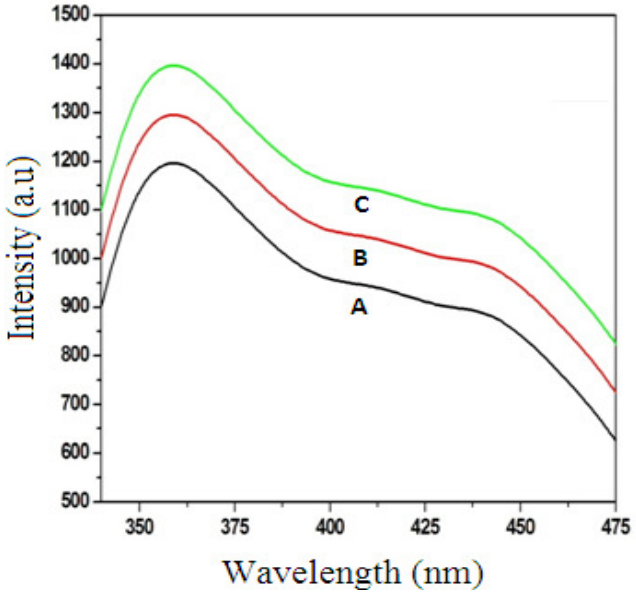

Figure-6
Photoluminescence spectra of ZnS nanoparticles A, B and C

FTIR Study: FTIR measurements are carried out to identify the possible biomolecules responsible for capping and efficient stabilization of the ZnS nanoparticles. For comparison we show the spectra for the pure *A.bisporus* extract (figure-7(a)) and for one representing sample (sample A) (figure-7(b)). The intense broad band in figure-7(a) at 3294 cm $^{-1}$ is due to N – H and O – H stretching mode in the linkage of the proteins[19], the medium intense band at 1638 cm $^{-1}$ arises from the C = O stretching mode in amide- I group which is commonly found in protein[20], the band at 1538 cm $^{-1}$ is due to –N – H stretching vibration in the amide-II linkage of protein[20] and the band at 2356 cm $^{-1}$ is due to O = C = O stretching vibration[2]. Figure-7 (b) displays all the functional groups present in the *A. bisporus* extract. A close comparison of the vibrational bands in these two figures reveals band shifting in figure-7(a) with respect to figure-7(b). The shift of these stretching frequencies indicates a bonding of the biomolecules to the ZnS nanoparticles through these groups. Thus the FTIR study has confirmed the presence of proteins as capping agent for ZnS nanoparticles which increases the stability of the nanoparticles synthesized. The peak appearing at 488 cm $^{-1}$ in figure-7(b) is due to Zn-S stretching vibration assigned to the ZnS band[3] (corresponding to sulphide). The FTIR peak assignments of these two samples are listed in table-3. In the mechanism of formation of ZnS, initially zinc sulphide is formed. When ZnS grows to a particular nano size it binds to protein and the latter is acting as a shield and prevents further growth and thereby every particle has to remain in the nano size. A. Ahmad et al.[20] have reported that proteins can bind to metal nanoparticles through the free amine groups or carboxylate ion of amino acid residues.

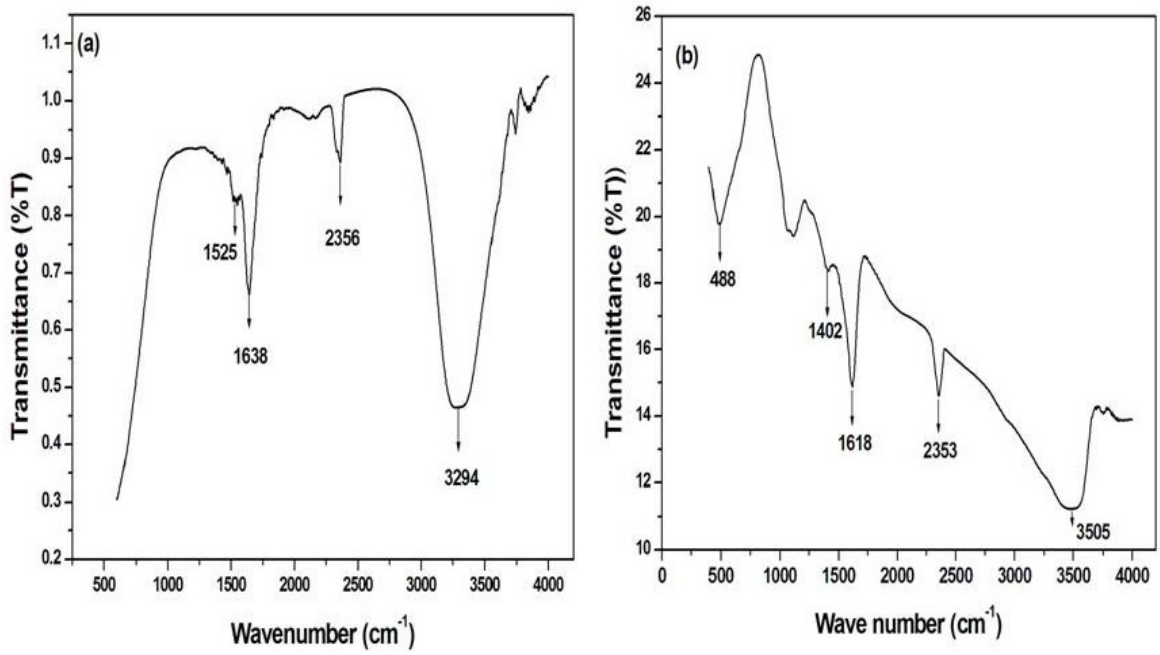

Figure-7
FTIR spectra of (a) *Agaricus bisporus* extract and (b) sample A

Table-3
IR Peaks and their assignments

A. bisporus extract		ZnS nanoparticles	
Position (cm^{-1})	Assignment	Position (cm^{-1})	Assignment
3294	O-H, N-H Stretching	3505	O-H, N-H Stretching
2356	O=C=O Stretching	2353	O=C=O Stretching
1638	C=O Stretching	1618	C=O Stretching
1525	-N-H Stretching	1404	-N-H Stretching
		488	Zn-S Stretching

Thermogravimetric study: Figure-8 shows the thermogravimetric (TGA) results of samples A, B and C. The 8% weight loss for sample A and 30% for samples B and C up to 300°C is due to the evaporation of residual moisture or solvent absorbed to the surface or inner of the samples. From 300°C – 500°C for sample A and from 300°C- 504°C for samples B and C there is no weight loss.

Impedance Study: Quantum dots are associated with capacitance and quantum dot admittance (or impedance) is basically due to capacitance present in the specimen[21]. Thus, capacitance (hence capacitive admittance) is a function of quantum dot size, shape and material[22]. To explore possibility of any such correlation in our samples, we carried out impedance analysis. To be particular, the variation of admittance (S), a parameter linked to inductance, with applied frequency at room temperature has been studied. These plots are shown in figure 9.

It is clear from the figure that with increase of frequency the

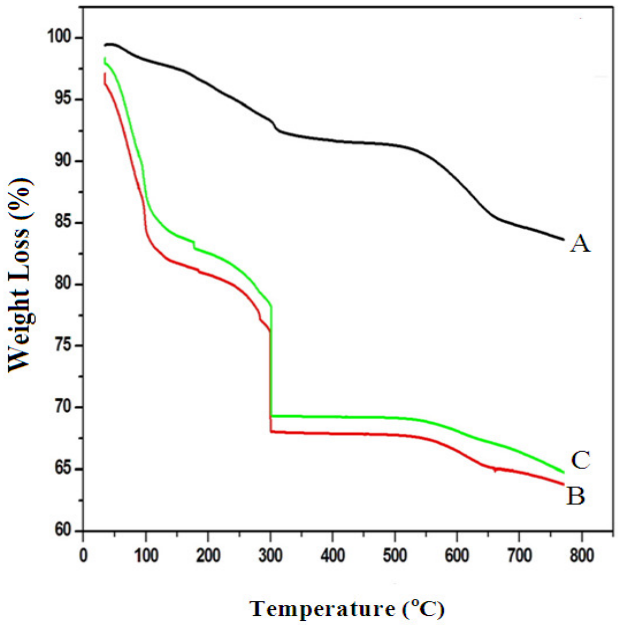

Figure-8
TGA spectra of samples A, B and C

admittance value is seen to rise first and then decrease after a critical frequency value. This nature is same for all the three samples. The critical frequency for these samples is 299.24 KHz. The reason for the fall in admittance is due to the loading effect of charge carriers. This is the property of electronic tuned

circuit and the frequency at which maximum admittance is attained may be compared to the resonant frequency of a conventional tuned circuit and this frequency may be called 'equivalent resonant frequency'[21]. It has been reported[22] that bulk ZnS does not show any variation in admittance. Therefore, these ZnS nanocrystals might have some application potential in nanotuned devices.

Comparisons of *A.bisporus* extract capped (present work) and *P.ostreatus* extract capped (our reported work[2]) ZnS nanoparticles: Table 4 shows a comparison between the *A.bisporus* extract capped ZnS nanoparticles (present work) and the *P.ostreatus* extract capped ZnS nanoparticles (our reported work[2]). It is observed from this table that crystallite and particle size of button mushroom extract capped ZnS nanoparticles are smaller than oyster mushroom extract capped ZnS nanoparticles. Also, the optical band gap values of button mushroom extract capped ZnS nanoparticles are much higher compared to oyster mushroom extract capped ZnS nanoparticles. It is to be noted that in both cases same amount of mushroom extract are being used. From the FTIR study of present work and our earlier work[2] it is found that protein containing in the mushroom extract is responsible for capping and stabilizing the ZnS nanoparticles. Md.A.Khan et al.[23] have reported that percentage of protein containing in oyster mushroom is 23.5% whereas F.Nasiri et al.[11] have reported that button mushroom contains 34.5% protein. Due to the presence of higher percentage of protein in button mushroom the interaction between the spherical ZnS nanoparticles and biomolecules present in the button mushroom extract is higher compared to spherical ZnS nanoparticles obtained by using oyster mushroom extract. Therefore, different properties ZnS nanoparticles are being obtained using same amount of button and oyster mushroom extract.

Conclusion

ZnS nanoparticles have been successfully synthesized at room temperature by a green chemical route using fresh *A. bisporus* extract. XRD patterns confirm the cubic crystalline structure of ZnS. Elemental analysis of ZnS nanoparticles confirms the presence of Zinc and Sulphur. The morphology of the particles has been identified from the SEM and TEM analysis reveals spherical shape particles with average particle size of 3.5-2.1 nm. The UV-vis. absorption peaks exhibit large blue shift and strong intensity. PL spectra show a broad peaks centred at 358 nm and weak shoulder at around 440 nm. The FTIR study confirms the presence of amide groups of protein which could bind with ZnS nanoparticles stopping agglomeration. TGA analysis show that samples B and C are more stable compared to sample A. Impedance analysis shows that admittance of samples A, B and C changes with change in frequency. Moreover, impedance analysis demonstrates that samples A, B and C can act as electronic tuned circuits with an equivalent resonance frequency of 299.247 KHz. A comparative study shows that the presence of different percentage of protein in button and oyster mushroom plays an important role in the properties ZnS nanoparticles.

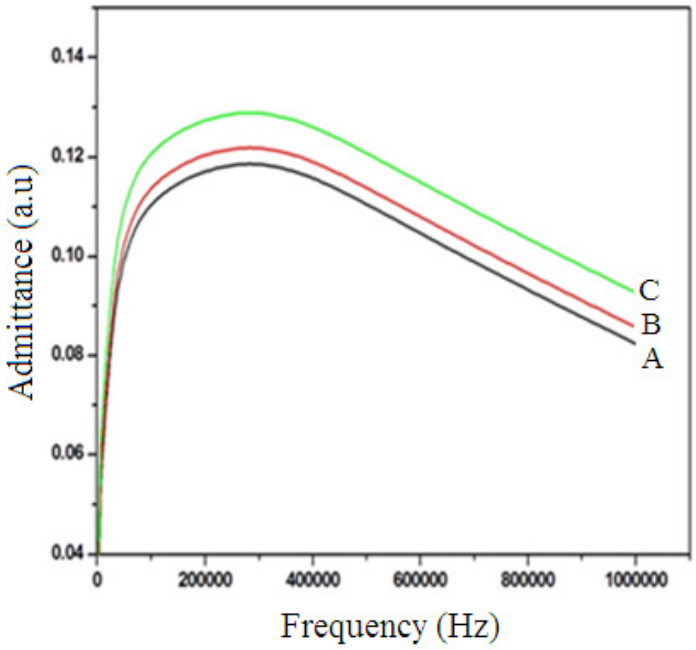

Figure-9
Variation of admittance of samples A, B and C with frequency

Table-4
Comparison of *A.bisporus* capped ZnS nanoparticles (present work) with *P.ostreatus* capped ZnS nanoparticles (our reported work[2])

Extract Volume (ml)	Crystallite Size (nm)		Particle Size (nm)		Band Gap (eV)	
	ZnS NP (Present work)	ZnS NP (reported work[2])	ZnS NP (Present work)	ZnS NP (reported work[2])	ZnS NP (Present work)	ZnS NP (reported work[2])
50	2.90	3.10	3.5	4.04	4.90	4.68
100	2.50	2.94	3.0	3.12	5.20	4.74
150	2.10	2.91	2.1	2.30	5.30	4.75

Acknowledgement

Authors gratefully acknowledge institute of biotech hub, Handique Girls' College, Guwahati for providing laboratory facilities.

References

1. Senapati U.S., Jha D.K. and Sarkar D., Green Synthesis and Characterization of ZnS nanoparticles, *Res. J. Physical Sci.*, **1(7)**, 1-6 **(2013)**

2. Senapati U.S. and Sarkar D., Characterization of biosynthesized zinc sulphide nanoparticles using edible mushroom pleuratuss ostratu, *Indian J. Phys*., **88**, 557-562 **(2014)**

3. Farooqi M.M.H. and Srivastava R.K., Structural, optical and Photoconductivity study of ZnS nanoparticles synthesized by a low temperature solid state reaction method, *Mater. Sci. Semicond. Process.,* **20**, 61-67 **(2014)**

4. Chai L., He Wen., Sun L., Jin F., Hu Xiang Yang. and Ma J., Solvothermal synthesis of wurtzite ZnS complex spheres with high hierarchy, *Mater. Lett.,* **120**, 26-29 **(2014)**

5. Mohanpuria P., Rana N.K. and Yadav S.K., Biosynthesis of nanoparticles: technological concepts and future applications, *J. Nanopart. Res.,* **10**, 507-517 **(2008)**

6. Bai Hong-Juan., Zhang Zhao-Ming. and Gong J., Biological synthesis of semiconductor zinc sulfide nanoparticles by immobilize Rhodobacter sphaeroides, *Biotechnol. Lett.,* **28,** 1135-1139 **(2006)**

7. Malarkodi C. and Annadurai G., A novel biological approach on extracellular synthesis and characterization of semiconductor zinc sulfide nanoparticles, *Appl. Nanosci.,* **3,** 389-395 **(2013)**

8. Philip D., Biosynthesis of Au, Ag and Au-Ag nanoparticles using edible mushroom extract, *Spectrochimica Acta Part A.,* **73**, 374-381 **(2009)**

9. Dhanasekaran D., Latha S., Saha S., Thajuddin N. and Panneerselvam A., Extracellular biosynthesis, characterization and in-vitro antibacterial potential of silver nanoparticles using Agaricus bisporus, *J.Expt. Nanosci.,* **8(4),** 579-588 **(2013)**

10. Bhat R., Sharanabasava V.G., Deshpande R., Shetti U., Sanjeev G. and Venkataraman A., Photo-bio-synthesis of irregular shaped functionalized gold nanoparticles using edible mushroom pleurotus florida and its anticancer evaluation, *J. Photochem. Photobio. B: Bio.,* **125**, 63-69 **(2013)**

11. Nasiri F., Tarzi B.G., Bassiri A. and Hoseini S.E., Comparative study on some chemical compounds of button mushrooms (Agaricus Bisporus) cap and stipe during the first and third flushes, *Annals Bio. Res.,* **3(12),** 5677-5680 **(2013)**

12. Kripal R., Gupta A.K., Mishta S.K., Srivastava K., Pandey A. C. and Prakash S.G., Photoluminescence and photoconductivity of ZnS:Mn^{+2} nanoparticles synthesized via co-precitation method, *Spectrochimica Acta Part A.,* **76**, 523-530 **(2010)**

13. Bilgin V., Kose S., Atay F. and Akyuz I., The effect of substrate temperature on the structural and some physical properties of ultrasonically sprayed CdS films, *Mater. Chem. phys.,* **94**, 103-108 **(2005)**

14. Hudlikar M., Joglekar S., Dhaygude M. and Kodam K., Latex-mediated synthesis of ZnS nanoparticles: green synthesis approach, *J.Nanopart. Res.,* **14**, 865 **(2012)**

15. Vogel W., Borse P. H., Deshmukh N. and Kulkarni S., Structure and stability of monodispersed 1.4 nm ZnS particles stabilized by mercaptoethanol, *Langmuir.,* **16(4),** 2032-2037 **(2000)**

16. Pathak C.S., Mandal M.K. and Agarwala V., Synthesis and characterization of zinc sulphide nanoparticles prepared by mechanochemical route, *Superlattice and Microstructure*., **58,** 135-143 **(2013)**

17. Ravindra N. M., Ganapathy P. and Choi J., Energy gap-refractive index relations in semiconductors- An overview, *Infrared Physics and Technology*., **50**, 21-29 **(2007)**

18. Bhattacharjee B. and Lu Chung-Hsin., Multicolor luminescence of undoped zinc sulfide nanocrystalline thin films at room temperature, *Thin Solid Films.,* **514,** 132-137 **(2006)**

19. Loo Y. Y., Chieng B. W., Nishibuchi M. and Radu S., Synthesis of silver nanoparticles by using tea leaf extract from camellia sinensis, *Int. J. Nanomedicine.* , **7**, 4263-4267 **(2012)**

20. Ahmad A., Senapati S., Khan M.I., Kumar R. and Sastry M., Extracellular biosynthesis of monodisperse gold nanoparticles by a novel extromophilic actinomycete, Thermomonospora Sp., *Langmuir.,* **19,** 3550-3553 **(2003)**

21. Bompilwar S. D., Kondawar S. B. and Tabhane V. A., Impedance study of nanostructure cadmium sulfide and zinc sulfide, *Arch. Apll. Sci. Res.,* **2(3),** 225-230 **(2010)**

22. Nath S. S., Chakdar D., Gopal G. and Avasthi D. K., Characterization of CdS and ZnS quantum dots prepared via a chemical method on S B R Latex, *Azajonano-J.Nanotechnology*., **4,** 1 **(2008)**

23. Khan Md. Asaduzzaman., Amin S.M.Ruhul., Uddin Md. Nazim., Tania M. and Alam N., Composition of oyster mushrooms cultivated in Bangladesh, *Bangladesh J. Mushroom.,* **2(1),** 9-14 **(2008)**